Chinese Journal of Natural Medicines

Ethanol extract of Cyathulae Radix inhibits osteoclast differentiation and bone loss

Liying SHI, Liuyi REN, Jinping LI, Xin LIU, Jingjing LU, Lujuan JIA, Baoping XIE, Siyuan TANG, Wei LIU, Jie ZHANG

Citation: Liying SHI, Liuyi REN, Jinping LI, Xin LIU, Jingjing LU, Lujuan JIA, Baoping XIE, Siyuan TANG, Wei LIU, Jie ZHANG, Ethanol extract of Cyathulae Radix inhibits osteoclast differentiation and bone loss, Chinese Journal of Natural Medicines, 2024, 22(3), 212−223. doi: 10.1016/S1875−5364(24)60596−0.

View online: https://doi.org/10.1016/S1875−5364(24)60596−0

Available online at www.sciencedirect.com
ScienceDirect
Chinese Journal of Natural Medicines 2024, **22**(3): 212-223
doi: 10.1016/S1875-5364(24)60596-0
Chinese Journal of Natural Medicines

•Original article•

Ethanol extract of Cyathulae Radix inhibits osteoclast differentiation and bone loss

SHI Liying[1Δ], REN Liuyi[1Δ], LI Jinping[1, 2*], LIU Xin[1], LU Jingjing[1], JIA Lujuan[1], XIE Baoping[3], TANG Siyuan[4], LIU Wei[4], ZHANG Jie[5]

[1] *Department of Pharmachemistry, Xiangya School of Pharmaceutical Sciences, Central South University, Changsha 410013, China;*
[2] *Hunan Key laboratory of Diagnostic and Therapeutic Drug Research for Chronic Diseases, Central South University, Changsha 410013, China;*
[3] *Key Laboratory of Prevention and Treatment of Cardiovascular and Cerebrovascular Diseases, Ministry of Education, Gannan Medical University, Ganzhou 341000, China;*
[4] *Xiangya Nursing School, Central South University, Changsha 410013, China;*
[5] *The Third Xiangya Hospital, Central South University, Changsha 410013, China*

Available online 20 Mar., 2024

[ABSTRACT] Cyathulae Radix, a traditional Chinese medicine and a common vegetable, boasts a history spanning millennia. It enhances bone density, boosts metabolism, and effectively alleviates osteoporosis-induced pain. Despite its historical use, the molecular mechanisms behind Cyathulae Radix's impact on osteoporosis remain unexplored. In this study, we investigated the effects and mechanisms of Cyathulae Radix ethanol extract (CEE) in inhibiting osteoporosis and osteoclastogenesis. Eight-week-old female mice underwent ovariectomy and were treated with CEE for eight weeks. Micro-computed tomography (micro-CT) assessed histomorphometric parameters, bone tissue staining observed distal femur histomorphology, and three-point bending tests evaluated tibia mechanical properties. Enzyme-linked immunosorbent assay (ELISA) measured serum estradiol (E_2), receptor activator for nuclear factor B ligand (RANKL), and osteoprotegerin (OPG) levels. Osteoclastogenesis-related markers were analyzed *via* Western blotting (WB) and quantitative real-time polymerase chain reaction (qRT-PCR). Additionally, CEE effects on RANKL-induced osteoclast formation and bone resorption were investigated in vitro using tartrate-resistant acid phosphatase (TRAP) staining, qRT-PCR, and WB assay. Compared with the ovariectomy (OVX) group, CEE treatment enhanced trabecular bone density, maximal load-bearing capacity, and various histomorphometric parameters. Serum E_2 and OPG levels significantly increased, while Receptor activator of nuclear factor-κB (RANK) decreased in the CEE group. CEE downregulated matrix metallopeptidase 9 (MMP-9), Cathepsin K (CTSK), and TRAP gene and protein expression. In bone marrow macrophages (BMMs), CEE reduced mature osteoclasts, bone resorption pit areas, and MMP-9, CTSK, and TRAP expression during osteoclast differentiation. Compared with DMSO treatment, CEE markedly inhibited RANK, TNF receptor associated factor 6 (TRAF6), Proto-oncogene c-Fos (c-Fos), Nuclear factor of activated T-cells cytoplasmic 1 (NFATc1) expressions, and Extracellular regulated protein kinases (ERK), c-Jun N-terminal kinase (JNK), NF-kappa B-p65 (p65) phosphorylation in osteoclasts. In conclusion, CEE significantly inhibits OVX-induced osteoporosis and RANKL-induced osteoclastogenesis, potentially through modulating the Estrogen Receptor (ER)/RANK/NFATc1 signaling pathway.

[KEY WORDS] Osteoporosis; Osteoclast; BMMs; Cyathulae Radix; RANKL; ER/RANK/NFATc1 signaling pathway
[CLC Number] R965 **[Document code]** A **[Article ID]** 2095-6975(2024)03-0212-12

Introduction

Osteoporosis, a systemic skeletal disorder, is characterized by compromised bone microstructure and diminished bone mass, quality, and strength, leading to an increased risk of fractures. The maintenance of bone integrity relies on the dynamic equilibrium between bone absorption and formation. Osteoclasts are pivotal in bone resorption, secreting acidic substances and enzymes that dissolve bone minerals, thereby contributing to bone loss. Osteoporosis manifests when the activity of osteoclasts surpasses that of osteoblasts, resulting in higher bone resorption than formation. Post-menopausal

[Received on] 03-Jun.-2023
[Research funding] This work was supported by the National Natural Science Foundation of China (Nos. 81273816, 81774379, and 81370974), the Natural Science Foundation of Hunan Province, China (Nos. 2017JJ2338 and 2020JJ4860), the Fundamental Research Funds for the Central Universities of Central South University (No. 502211706), and the Fund for the Key Laboratory of Hunan Province, China (No. 2017TP1004).
[*Corresponding author] E-mail: pjingli@163.com
ΔThese authors contributed equally to this work.
These authors have no conflict of interest to declare.

women, particularly in the 5−10 years after menopause, experience a decrease in estrogen levels due to ovarian endocrine dysfunction or decline, enhancing osteoclast bone resorption capacity and leading to post-menopausal osteoporosis [1, 2].

In osteoporosis diagnosis and treatment, osteoclast-related indices are frequently utilized. Various factors regulate osteoclast differentiation, maturation, and function, involving complex and intertwined signaling pathways. The receptor activator for nuclear factor B ligand (RANKL) is crucial for osteoclast differentiation, and the osteoprotegerin (OPG)-RANKL-RANK signaling pathway plays a significant role in osteoclast formation and differentiation [3]. M-CSF fosters osteoclast differentiation and enhances the interaction between RANK and RANKL [4–6]. RANK, lacking intrinsic kinase activity for phosphorylation and activation of downstream signaling molecules, recruits TRAF6 upon binding with RANKL, thereby activating downstream pathways such as NF-*κ*B, MAPK, and c-src-PI3K-Akt signaling pathways [7, 8]. NF-*κ*B, a key regulator of mature osteoclast survival and function, promotes osteoclast differentiation and prevents apoptosis after entering the nucleus [9]. In its resting state, NF-*κ*B tightly binds to the inhibitor I*κ*B in the form of p50/p65. The early upregulation of I*κ*Bα expression initiates a negative feedback loop, limiting the intranuclear translocation of p65/p50 [10]. The MAPK signaling pathway, encompassing ERK, JNK, and p38 pathways, is also implicated. Activation of these MAPK pathways increases the expression of NFATc1, promoting the differentiation and function of mature osteoclasts [11–14]. Blocking the p38 pathway can inhibit osteoclast differentiation, maturation, and local bone resorption [15]. GSK3β prevents NFATc1 from binding to DNA [16], and Akt activation can block GSK3β [17]. Activation of these pathways transmits signals to c-Fos and NFATc1, influencing osteoclast formation [18, 19]. NFATc1, a crucial transcriptional regulator in osteoclasts, translocates from the cytoplasm to the nucleus upon activation, inducing transcription of osteoclast-specific genes such as tartrate resistant acid phosphatase (*Trap*), Cathepsin K (*Ctsk*) and matrix metallopeptidase 9 (*Mmp-9*) [20]. Estrogen receptor α (ERα) is vital for the anti-osteoporotic role of estrogen, inhibiting osteoclast differentiation by downregulating RANK [21].

Cyathulae Radix, documented in the *Pharmacopoeia of the People's Republic of China*, is the dry root of *Cyathula officinalis* Kuan. It is a common traditional Chinese medicine used to treat various orthopedic diseases, such as bone injury, osteoarthritis, and rheumatic arthritis [22]. It is also a traditional vegetable in China. Recognized as a dietary supplement by the National Health Commission of the People's Republic of China, Cyathulae Radix has extensive pharmacological effects, including effects on growth and articulation, as well as anti-inflammatory, antioxidant, antihypertensive, and antitumor effects [23]. WANG *et al*. [24] revealed that Cyathulae Radix exerts a weak estrogen-like effect in ovariectomized rats, potentially contributing to the treatment of osteoporosis. Additionally, it also displays osteoprotective effects in ovariectomized rats [25]. The main constituents of Cyathulae Radix are triterpenoid saponins, steroid ketones, and polysaccharides. Steroid ketones, including ecdysterone and cystinone, have been shown to possess anti-osteoporotic effects [26, 27]. Estrogen deficiency is the main cause of post-menopausal osteoporosis. Cyasterone, an authentic standard found in Cyathulae Radix extract, not only exhibits significant estrogen-like effects but also notably inhibits osteoclastic differentiation and promotes osteogenic differentiation [28]. Triterpenoid saponins, mainly cyanoside A and B, along with polysaccharides in Cyathulae Radix, have demonstrated anti-inflammatory activity [29]. Polysaccharides can downregulate the proportion of $CD4^+CD25^+Foxp3^+$Tregs cells [30]. However, the molecular mechanisms underlying the effects of Cyathulae Radix on osteoporosis remain unexplored.

Therefore, the objective of this study was to explore the preventive and therapeutic effects of Cyathulae Radix ethanol extract (CEE) *in vitro* and *in vivo*. It will significantly benefit the development and utilization of Cyathulae Radix.

Materials and Methods

Preparation of CEE and estradiol (E_2)

Cyathulae Radix was purchased from Hengyue Herbal Pieces Co., Ltd. (Hengyang, China, Lot: 17101304). The raw material was subjected to extraction twice, each for 2 h, using 30-fold ethanol (70%, *V*/*V*) at 85 °C. The resultant solution was concentrated, following which polysaccharides were removed, and the ethanol evaporated to dryness. CEE was then reconstituted in water to achieve the desired concentrations: 4.76 mg·mL^{-1} for the high dose (HD) and 1.19 mg·mL^{-1} for the low dose (LD) in mice. DMSO was added to dissolve and dilute the CEE for cell culture.

For the preparation of E_2, 1 mg of an E_2 valerate tablet (Bayer China, Lot: 395A) was ground into powder. The powder was then diluted in water to a concentration of 0.03 mg·mL^{-1} for use in mice.

High-performance liquid chromatography (HPLC) analysis

CEE was filtered using a Millipore syringe filter (0.45 μm, 50 mm, PES). All compounds in the extract were determined using the LC-2010AHT HPLC System (Shimadzu, Kyoto, Japan). HPLC analyses were performed on a reverse phase Gensial® C_{18} column (250 mm × 4.6 mm, 5 μm). The mobile phase consisted of 0.2% acetic acid in water (A) and methanol (B) using a linear gradient program: from 70% A at 0 min to 55% A over 10−40 min, and then to 5% A from 40 to 50 min. The flow rate was maintained at 1 mL·min^{-1}, and the injection volume was set at 10 μL. The column temperature was controlled at 35 °C, and detection was performed at a wavelength of 243 nm (Fig. S1).

For the quantification of Cyasterone in CEE, an accurately weighed amount of Cyasterone (2.03 mg) was dissolved in 10 mL of methanol, generating a series of concentrations for analysis. A calibration curve was plotted based on the peak-area ratio of Cyasterone against its molar ratio, fol-

lowing the equation: $Y = 9264.2X + 11\,216$, $R^2 = 0.9998$; 5.075−81.200 μg·mL^{-1}. The concentration of Cyasterone in CEE was determined to be over 1.05%.

Cell cultures and toxicity assessment

Bone marrow macrophages (BMMs) were extracted from the femora and tibias of 5-week-old female C57BL/6 mice. The bone marrow cavities were flushed with α-MEM to harvest bone marrow cells. These cells were then cultured in α-MEM supplemented with 10% fetal bovine serum (FBS), 100 U·mL^{-1} penicillin and 100 μg·mL^{-1} streptomycin (Solarbio, USA) at 37 °C in a 5% CO_2 atmosphere. After 12 h, the non-adherent cells were collected and subsequently cultured with macrophage colony-stimulating factor (M-CSF, 30 ng·mL^{-1}) for 4 d. BMMs were treated with RANKL (50 ng·mL^{-1}) and M-CSF (30 ng·mL^{-1}) for 4−6 d to induce osteoclast formation. During this induction phase, varying concentrations of CEE and 5 μmol·L^{-1} E_2 were added to intervene in osteoclast induction, respectively.

The cytotoxic effects of CEE on BMMs were evaluated using the CCK-8 assay. After BMMs were seeded in 96-well plates for 24 h, they were exposed to different concentrations of CEE (0.025, 0.050, 0.100, 0.125, 0.150, and 0.300 mg·mL^{-1}). Following a 48-h incubation, CCK-8 reagent was added to the culture medium, and the plates were further incubated for 3 h at 37 °C in a 5% CO_2 environment. The optical density of each well was measured at a wavelength of 450 nm using a microplate reader.

TRAP staining

BMMs were treated with RANKL (50 ng·mL^{-1}) and M-CSF (30 ng·mL^{-1}) for 6 d to induce osteoclast formation. Post-induction, the cells were washed with PBS buffer and fixed in 4% paraformaldehyde. Staining was then performed using a TRAP staining kit according to the manufacturer's instructions. TRAP-positive cells containing three or more nuclei were identified as osteoclasts. These cells were subsequently counted under an inverted microscope (NIS-Elements F 4.0).

Pit formation assay

BMMs stimulated by M-CSF and RANKL were cultured on bovine bone slices (thickness: 100−200 μm) to evaluate pit formation in the presence or absence of CEE. Following an 8-day culture, these bone slices were washed with PBS and fixed in 4% paraformaldehyde for 20 min. The bone slices were then stained with toluidine blue dye (Sloarbio, China) for 10 min. Resorption pits were imaged using an inverted microscope, and their areas were quantified using Image-Pro-Plus 6.0 software.

Animals and experimental procedures

In total, 60 female ICR mice (Hunan SJA Laboratory Animal Co., Ltd.) were acclimated to a specific pathogen-free (SPF) environment at the research animal laboratory. 8-week-old female mice were randomly assigned to six groups (n = 10/group) for subsequent oral gavage treatments: Blank, SHAM-operated (SHAM), OVX-mice (OVX), OVX-mice treated with 0.03 mg·mL^{-1} E_2 (OVX-E_2), OVX-mice treated with 1.19 mg·mL^{-1} CEE (OVX-LD), OVX-mice treated with 4.76 mg·mL^{-1} CEE (OVX-HD). The Blank group received no treatment. Fat around ovaries were removed from mice in the SHAM group, while bilateral ovaries were removed from mice in other groups. All mice were monitored for eight weeks post-surgery and treatment, after which they were humanely euthanized for the collection and analysis of serum, tibias, and femora. This study's protocols were in strict adherence to ethical standards and national guidelines for animal care and use, approved by the Animal Experimentation Ethics Committee of Central South University (Ref. No. 2018sydw0207).

Micro-computed tomography (Micro-CT) analysis

The left femora of mice were taken, and bone trabecula in the distal femoral metaphysis was measured by micro-CT [NEMO® Micro-CT, PINGSENG Healthcare (Kunshan) Inc., China]. The scanning targeted the bone trabeculae within the distal femoral metaphysis. The defined scanning area was the distal metaphysis, extending 1 mm proximally from the growth plate, followed by three-dimensional reconstruction. Key indices assessed included bone volume (BV), structural model index (SMI), bone mineral contents (BMC), bone volume fraction (BV/TV), bone surface area to tissue volume ratio (BS/TV), bone surface area to bone volume ratio (BS/BV), and trabecular bone thickness (Tb.Th). The scanning parameters were set as follows: a sweep length of 0.5 mm, a voltage of 60 kV, a current of 200 μA, and reconstruction using an iterative algorithm [31, 32].

Histological analysis

Post-collection, the femora were fixed in 4% paraformaldehyde, decalcified using 10% EDTA, and subsequently embedded in paraffin. Longitudinal sections of 5 μm thickness were prepared and stained with Hematoxylin and Eosin (H&E) to examine the histomorphology of the distal femur. Images of these sections were captured using an M565 J/E/G Fluorescence inverted microscope (Nikon, Japan) [33, 34].

Mechanical properties testing

A three-point bending test was used to detect the mechanical properties of the tibias on an MTS Insight 30 biomechanics tester (MTS Industrial Systems Co., Ltd., USA), with the bones positioned across a 2 cm span. Tibias were subjected to transverse pressure at the midpoint at a constant rate of 1 mm/min until broken. Ultimate force (N) was calculated based on the collected load and displacement data.

Enzyme-linked immunosorbent assay (ELISA)

The blood sample was obtained and centrifugated to separate the serum. The levels of E_2, RANKL, and OPG in serum were measured using an ELISA kit (BangYi, Shanghai, China), strictly adhering to the manufacturer's protocol.

Quantitative real-time polymerase chain reaction (qRT-PCR)

Femora were flash-frozen in liquid nitrogen and ground to a fine powder. Total RNA was extracted from both femora and osteoclasts using TRIzol reagent (Invitrogen) following the manufacturer's protocol. Subsequent reverse transcription PCR was performed with 1.0 μg total RNA, and cDNA

was synthesized using a kit (Thermo Fisher Scientific, USA). qRT-PCR was then performed using specific primers listed in Table S1.

Western blotting (WB) assay

Proteins were extracted from the femora using TRIzol agent following the manufacturer's protocol. Cell lysates were prepared using RIPA Lysis Buffer, and protein concentrations were quantified *via* the BCA method. Protein samples (30 μg) were separated on SDS-PAGE gels and transferred to PVDF membranes. These membranes were blocked in either 5% BSA or 5% skim milk for 2 h and incubated overnight at 4 °C with primary antibodies against TRAP, CTSK (Novus, USA), MMP-9 (R&D, USA), RANK, ERα, c-Fos, NFATc1, p-Akt, p-p65, p-ERK, p-JNK, p-p38, p-IκBα, Akt, p65, ERK, JNK, p38, IκBα (CST, USA), GAPDH (Proteintech, USA), and TRAF6 (Abcam, USA), followed by a 2-hour room temperature incubation with appropriate secondary antibodies. The blots were visualized using an enhanced chemiluminescence (ECL) kit.

Statistical analysis

Each experiment was repeated at least three times, and all quantitative data were expressed as mean ± SD. Statistical analyses were conducted by one-way analysis of variance (ANOVA) and Student's *t*-test using IBM SPSS Statistics 22.0. A *P*-value < 0.05 was considered statistically significant.

Results

CEE suppressed osteoclast differentiation and bone-resorbing activity

CEE (0.025, 0.050, 0.100, 0.125, 0.150, and 0.300 mg·mL^{-1}) had no effect on the proliferation of BMMs (Fig. 1A). CEE at various concentrations (0.075, 0.150, and 0.3 mg·mL^{-1}) were used in the further research. Mouse BMMs were treated with M-CSF (30 ng·mL^{-1}) and RANKL (50 ng·mL^{-1}) to verify the effect of CEE on osteoclastogenesis. Post-treatment, TRAP staining identified mature TRAP-positive multinucleate osteoclasts, which were dyed wine red (Fig. 1B). Compared with that in the blank group, the number of mature osteoclasts increased notably in the RANKL-induced group. In contrast, CEE treatment reduced the formation and number of osteoclasts in a dose-dependent manner (P < 0.001, Fig. 1C).

CEE's effects on the bone-resorption activity of mature osteoclasts were also evaluated. While 0.150 mg·mL^{-1} CEE had no effect on osteoclast survival (Fig. 1A), it substantially reduced the area of resorption pits (P < 0.01, Figs. 1D−1E), suggesting that CEE decreases the bone-resorbing activity of mature osteoclasts without affecting their viability.

CEE suppressed the expressions of Mmp-9, Ctsk, and Trap of osteoclasts

The impact of CEE on the expression levels of *Mmp-9*, *Ctsk*, and *Trap* in osteoclasts was detected by qRT-PCR and WB analyses (Fig. 2). The gene expressions of *Ctsk*, *Mmp-9*, and *Trap* increased significantly over a period of 4−6 d. Compared with the DMSO group, the gene expressions of *Ctsk*, *Mmp-9*, and *Trap* decreased significantly within 2−4 d, the gene expressions of *Ctsk* and *Mmp-9* in CEE-treated groups and E_2 group decreased significantly on the 6th day (Fig. 2A). Notably, the 0.300 mg·mL^{-1} CEE group exhibited a notable reduction in *Trap* gene expression compared with the DMSO group (P < 0.01), but there were no statistically significant differences between the DMSO group and 0.150, 0.075 mg·mL^{-1} CEE group and E_2 group (P > 0.05). The gene expressions of *Mmp-9* and *Trap* were dose-dependent. The above results suggested that CEE can notably inhibit the gene expressions of *Ctsk*, *Mmp-9*, and *Trap*.

As shown in Fig. 2B, the protein expressions of MMP-9, CTSK, and TRAP in the DMSO group were significantly higher than those in the Blank group (MMP-9: P < 0.001, CTSK: P < 0.01, TRAP: P < 0.001). The expressions of osteoclast marker proteins in the 0.300 mg·mL^{-1} CEE group were significantly lower than those in the DMSO group (MMP-9: P < 0.001, CTSK: P < 0.05, TRAP: P < 0.001). The above results indicated that CEE significantly inhibits the protein expressions of MMP-9, CTSK, and TRAP in osteoclasts.

CEE inhibited the expressions of RANK, TRAF6, c-Fos, and NFATc1 in osteoclasts

Rank gene expression in the 0.075 mg·mL^{-1} CEE group was significantly lower than that in the DMSO group and 0.300 mg·mL^{-1} CEE group (P < 0.05). It was lower in the 0.075 mg·mL^{-1} CEE group than in the E_2 group and 0.150 mg·mL^{-1} CEE, but the difference was not statistically significant (P > 0.05, Fig. 3A). *Erα* gene expression in the 0.300 mg·mL^{-1} CEE group and E_2 group was markedly elevated compared with that in the DMSO group (0.300 mg·mL^{-1} CEE group: P < 0.001, E_2 group: P < 0.01). Furthermore, *Erα* gene expression in the 0.300 mg·mL^{-1} CEE group was significantly higher than in 0.150, 0.075 mg·mL^{-1} CEE groups and E_2 group (0.150, 0.075 mg·mL^{-1} CEE group: P < 0.001, E_2 group: P < 0.01, Fig. 3B). *Nfatc1* gene expression in CEE-treated groups were significantly lower than that in the DMSO group, (P < 0.001, Fig. 3C).

As shown in Figs. 3D−3E, the protein expressions of RANK, ERα, c-Fos, and NFATc1 were significantly higher in the DMSO group than those in the Blank group (RANK: P < 0.001, ERα, c-Fos, and NFATc1: P < 0.01). While ERα protein expressions in the DMSO group and CEE-treated groups were significantly higher than those in the Blank group, the difference was not statistically significant between the DMSO and CEE-treated groups, suggesting that CEE's inhibition of osteoclast differentiation may not be mediated through the upregulation of ERα expression. The protein expressions of RANK, c-Fos, and NFATc1 decreased significantly in the 0.300 mg·mL^{-1} CEE group (RANK and NFATc1: P < 0.001, c-Fos: P < 0.01). Additionally, the expression of TRAF6 decreased significantly in the 0.300 mg·mL^{-1} CEE group (P < 0.05), but no such significant change was observed in the 0.150 mg·mL^{-1} CEE group. These findings demonstrate that CEE can remarkably inhibit the protein expressions of RANK, TRAF6, c-Fos, and NFATc1 in osteoclasts.

CEE inhibited the phosphorylation levels of ERK, JNK, and p65

Groups were treated with CEE for 4 h and then stimulated with RANKL at various time points (0, 5, 15, 30, and 60 min) to detect the effect of CEE on total and phosphorylated protein levels of key molecules in different signaling pathways.

As shown in Fig. 4, CEE treatment significantly inhibited the phosphorylation of JNK at 15 min ($P < 0.001$), ERK at 5, 30, and 60 min (5 min: $P < 0.001$, 30 and 60 min: $P < 0.05$), and p65 at 0, 5, and 15 min ($P < 0.05$) compared with DMSO treatment, but no significant differences were observed at other time points ($P > 0.05$). The phosphorylation levels of IκBα, p38, and Akt had no significant changes at any time point compared with those in the DMSO group. The total protein levels of JNK increased significantly at 0 and 30 min ($P < 0.05$) and p65 and Akt at 0 min in the CEE group (p65: $P < 0.001$, Akt: $P < 0.05$) Other signaling molecules did not exhibit significant changes in total protein levels. These results suggest that CEE inhibits osteoclast differentiation by inhibiting the phosphorylation of ERK, JNK, and p65 rather than regulating the total protein expressions.

CEE inhibited ovariectomy-induced bone loss

Micro-CT was used to assess bone mass in mice with OVX-induced osteoporosis. The region of interest and longitudinal sections are depicted in Fig. 5B. As shown in Figs. 5A,

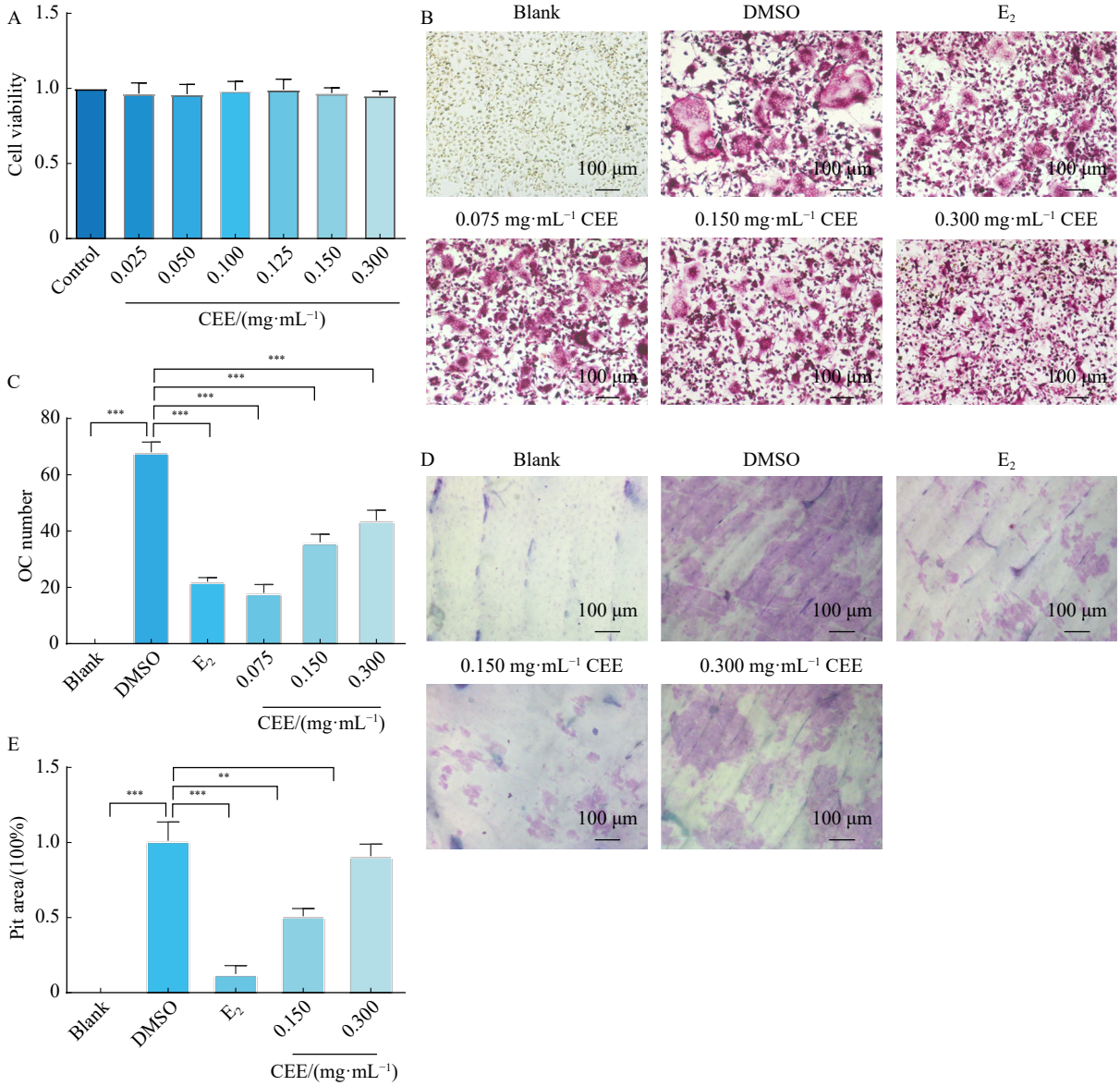

Fig. 1 CEE inhibited osteoclast differentiation and bone-resorbing activity in BMMs. (A) CEE in the test dose had no effect on the proliferation of BMMs. (B) The mature osteoclasts of each group were stained with TRAP staining. (C) CEE reduced the number of osteoclasts. (D) The bone slices of each group were stained with toluidine blue dye. (E) CEE decreased the bone-resorbing activity of mature osteoclasts. Data are expressed as the mean ± SD ($n = 3$). $^{*}P < 0.05$, $^{**}P < 0.01$, $^{***}P < 0.001$ *vs* DMSO group.

5C, and 5D, the OVX group, bone mass exhibited significantly reduced bone mass compared with those in the Blank and SHAM groups, with bone trabeculae appearing thinner and less dense. CEE treatment led to an increase in bone mass, with thicker and more abundant trabeculae.

BV/TV was significantly higher in the OVX-HD group than in the OVX group ($P < 0.05$, Fig. 5E). While the OVX-LD and OVX-E_2 groups also showed improvements in BV/TV, these were not statistically significant ($P > 0.05$). As shown in Fig. 5F, Tb.Th was significantly higher in all CEE-treated and OVX-E_2 groups than in the OVX group (OVX-HD group: $P < 0.05$, OVX-LD group: $P < 0.01$, OVX-E_2 group: $P < 0.001$, respectively). BV/TV and Tb.Th were higher in the OVX-HD group than in the OVX-LD, but the differences were not statistically significant. As depicted in Figs. 5G and 5H, BS/BV and SMI were significantly lower in the CEE-treated groups than in the OVX group ($P < 0.001$, $P < 0.05$, respectively). Compared with the OVX group, the CEE-treated groups exhibited no significant differences in BV, BMC, and BS/TV, although a gradual increase was noted ($P > 0.05$, Figs. 5I−5K).

CEE increased the maximal loads of tibias in OVX mice

The maximum load-bearing capacity was tested by a three-point bending test. The results, illustrated in Fig. 5L, demonstrated that the maximal load-bearing capacity of the tibia in the OVX group was significantly lower than that in the SHAM group ($P < 0.05$). In contrast, the maximum loads in the OVX-HD, OVX-LD, and OVX-E_2 groups showed a significant increase relative to the OVX group ($P < 0.05$). Although the maximum load in the OVX-E_2 group was marginally higher than that in the CEE-treated groups, this difference did not reach statistical significance ($P > 0.05$). Additionally, no significant differences in the maximum load were observed between the OVX-HD and OVX-LD groups ($P > 0.05$).

CEE upregulated E_2 and OPG levels and downregulated RANKL levels in serum

The levels of RANKL, E_2, and OPG in the serum of mice were quantitatively analyzed (Figs. 6A−6C). Compared with the OVX group, the SHAM and OVX-HD groups exhibited

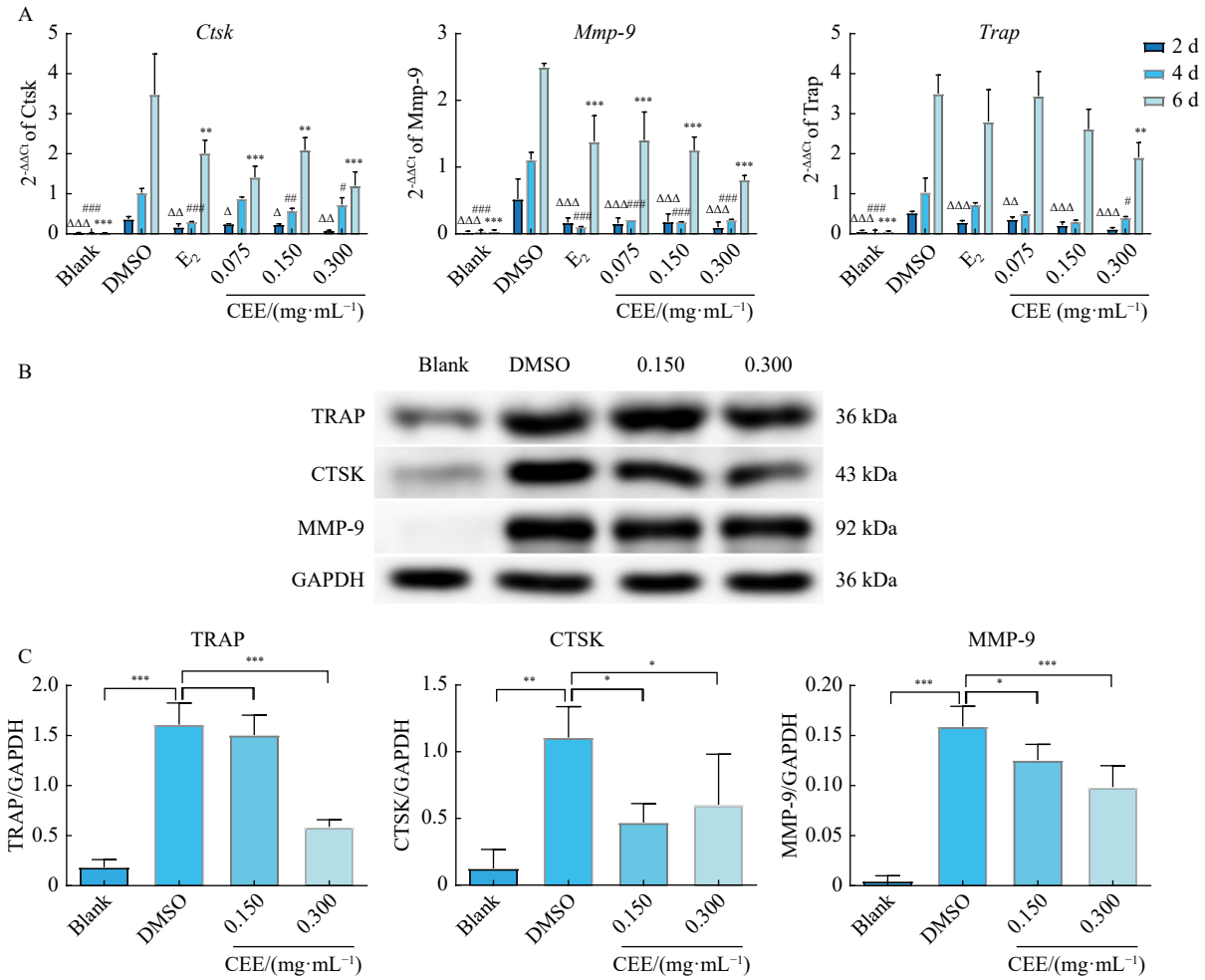

Fig. 2 CEE significantly inhibited the expressions of MMP-9, CTSK, and TRAP in osteoclasts. (A) Effect of CEE on gene expressions of *Ctsk*, *Mmp-9*, and *Trap*. (B) WB bands of TRAP, CTSK, MMP-9 and GAPDH. (C) Protein expressions of TRAP, CTSK, and MMP-9. Data are expressed as the mean ± SD ($n = 3$). Compared with the DMSO group, $^{▲}P < 0.05$, $^{▲▲}P < 0.01$, $^{▲▲▲}P < 0.001$; $^{\#}P < 0.05$, $^{\#\#}P < 0.01$, $^{\#\#\#}P < 0.001$; $^{*}P < 0.05$, $^{**}P < 0.01$, $^{***}P < 0.001$.

significant increases in the levels of E_2 and OPG (E_2: $P < 0.05$, OPG: $P < 0.01$, Figs. 6A and 6C) and a marked decrease inRANKL levels ($P < 0.001$, Fig. 6B). The OVX-LD group displayed higher levels of RANKL, E_2, and OPG than the OVX-HD group, but the differences were not statistically significant ($P > 0.05$). Furthermore, there were no significant differences in E_2 levels between the OVX-E_2 group and OVX-HD group ($P > 0.05$).

CEE inhibited the MMP-9, CTSK, and TRAP expressions of OVX mice

The levels of osteoporosis-related genes in mouse femur were detected by qRT-PCR, and the protein expression levels were detected by WB (Fig. 7). In the OVX group, the gene and protein expression levels of TRAP, CTSK, and MMP-9 in the femora were significantly higher than those in the Blank and SHAM groups. However, both gene and protein

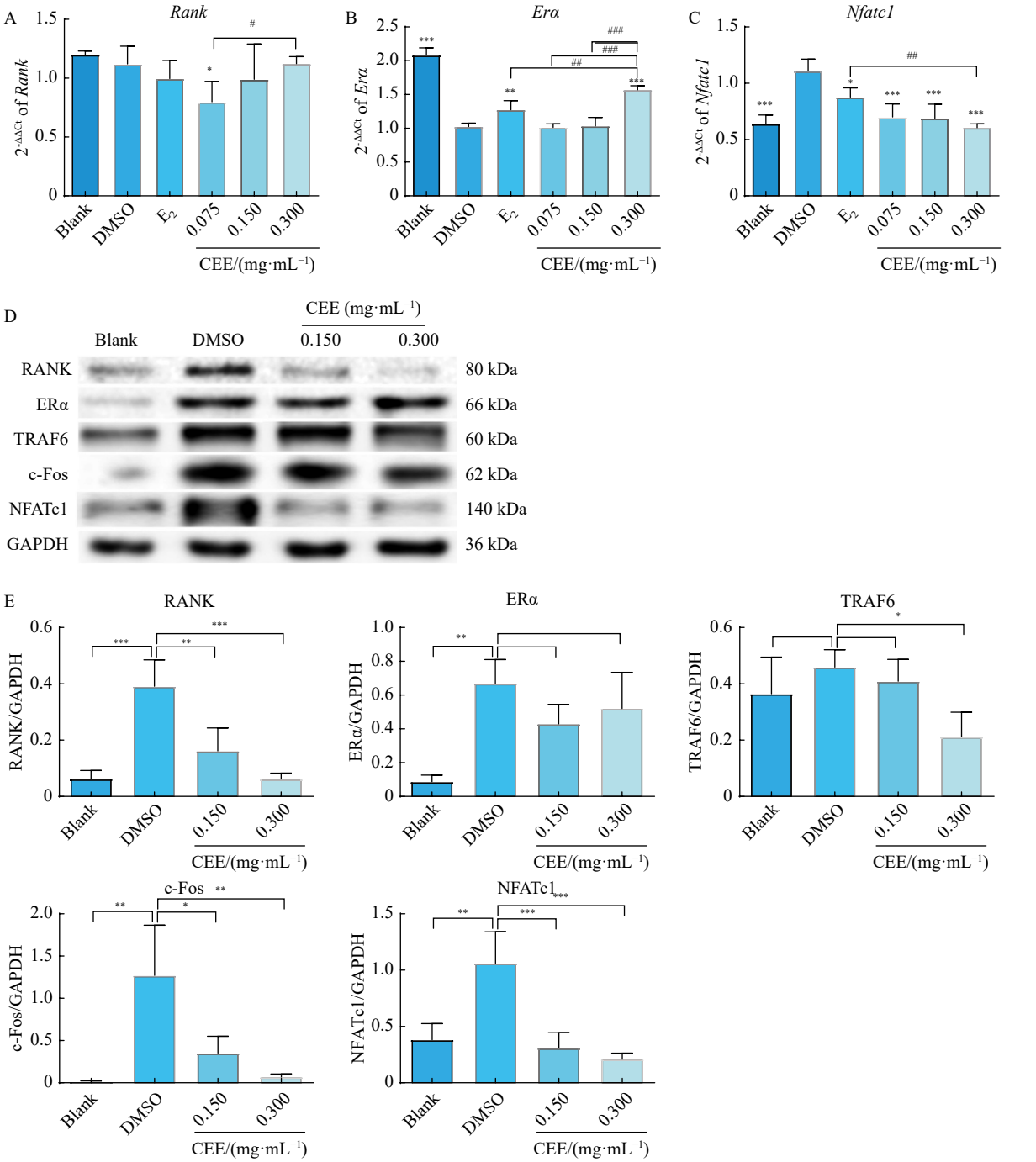

Fig. 3 CEE inhibited the expressions of key signaling molecules in osteoclasts. (A) Gene expression of *Rank*. (B) Gene expression of *Erα*. (C) Gene expression of *Nfatc1*. (D) WB bands of RANK, ERα, TRAF6, c-Fos, NFATc1, and GAPDH. (E) Effect of CEE on protein expressions of key signaling molecules. Data are expressed as the mean ± SD ($n = 3$). $^{*}P < 0.05$, $^{**}P < 0.01$, $^{***}P < 0.001$ *vs* DMSO group; $^{\#}P < 0.05$, $^{\#\#}P < 0.01$, $^{\#\#\#}P < 0.001$ *vs* 0.3 mg·mL^{-1} CEE group.

expression levels of TRAP, CTSK, and MMP-9 were significantly reduced in the CEE-treated groups and the OVX-E_2 group relative to the OVX group. There were no significant differences in gene expressions among the OVX-E_2, OVX-HD, and OVX-LD groups ($P > 0.05$, Fig. 7A). The protein expressions of CTSK and TRAP in the OVX-HD group were significantly higher than those in the OVX-LD and OVX-E_2 groups ($P < 0.001$). Meanwhile, MMP-9 protein expression in the OVX-HD group was higher than in the OVX-LD and OVX-E_2 groups, but this difference did not reach statistical significance ($P > 0.05$, Fig. 7C).

Discussion

As the population ages, the escalating prevalence of osteoporosis has imposed a substantial economic and health burden on society. Addressing the effective prevention and treatment of osteoporosis is thus an urgent concern in Chinese society. Currently, the primary treatment modalities for osteoporosis and other bone loss diseases include hormone replacement therapy (HRT) and bisphosphonates. However, these therapies are limited in their efficacy and associated with numerous adverse reactions [35]. In response to these limitations, Traditional Chinese medicine has gained increasing acceptance due to its effectiveness in disease treatment and lower side effect profile [36]. Recent scientific reports suggest that many natural herbal therapies have both anabolic and anticatabolic effects, making them beneficial for the treatment of osteoporosis by promoting bone formation and reducing unbalanced bone resorption [37, 38]. Notably, cyasterone, a key active component of Cyathulae Radix, has

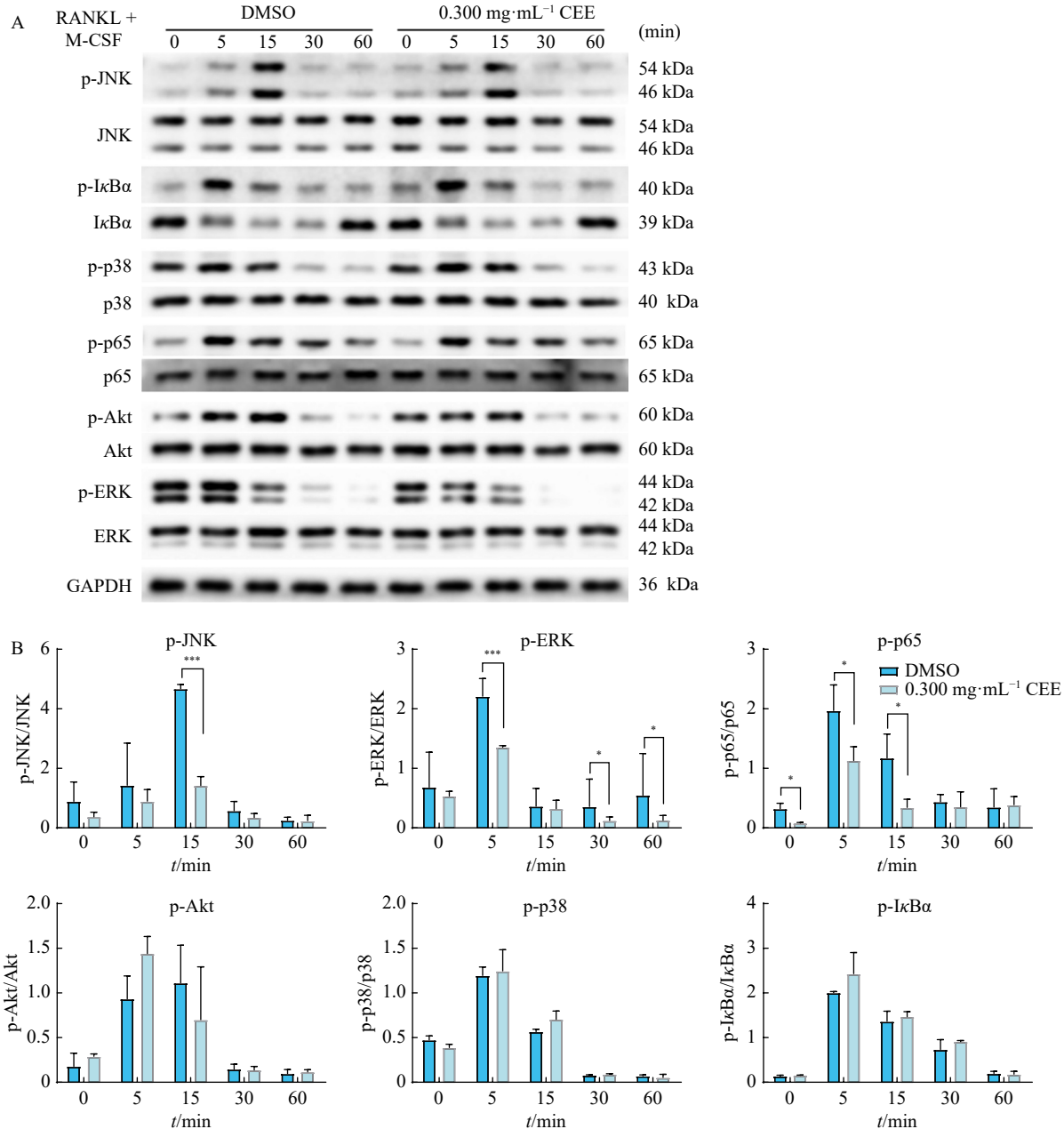

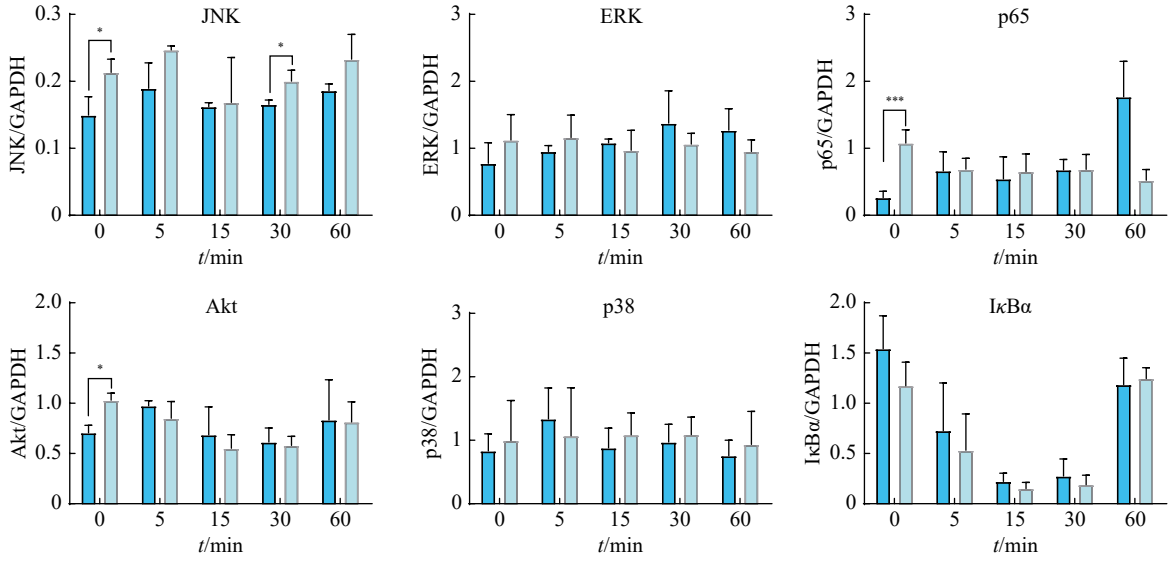

Fig. 4 CEE inhibited the phosphorylation levels of ERK, JNK, and p65. (A) Total and phosphorylated protein bands of key molecules in osteoclast signaling pathways. (B) Total protein and phosphorylation levels of key signal molecules in osteoclast differentiation. Data are expressed as the mean ± SD (n = 3). $^{*}P < 0.05$, $^{**}P < 0.01$, $^{***}P < 0.001$ *vs* DMSO group.

been found to counter osteoporosis by inhibiting osteoclastic differentiation and enhancing osteogenic differentiation [27].

The overactivation of osteoclasts plays a central role in various bone diseases, such as osteoporosis, rheumatoid arthritis, periprosthetic osteolysis, and periodontitis [39]. Natural Chinese medicine, in this context, can enhance bone formation activity and significantly inhibit bone resorption, potentially correcting the imbalance between osteoblast-mediated bone formation and osteoclast-mediated bone resorption [37]. Recently, targeting osteoclasts has become a forefront therapeutic strategy in the treatment of osteoporosis. The molecular regulation of osteoclast formation and function represents an important research area in developing osteoporosis treatments [40]. Therefore, the present study investigates the effect and mechanism of CEE in inhibiting osteoporosis and osteoclastogenesis. The research spans animal models, cell culture, and molecular biology, with a particular focus on the ER/RANK/NFATc1 signaling pathway.

In the ER/RANK/NFATc1 signaling pathway, estrogen predominantly modulates bone metabolism by interacting with ERα, known to inhibit the expression of RANK. Our findings reveal that CEE considerably suppresses the protein expressions of RANK and TRAF6 in osteoclasts, yet it does not significantly affect the protein expression of ERα. Furthermore, upon the binding of RANKL to RANK, TRAF6 attaches to the cytoplasmic region of RANK, initiating a cascade in the downstream signaling pathways, including NF-κB, MAPK, and c-src-PI3K-Akt. The MAPK signaling pathway comprises ERK, JNK, and p38 pathways. The data indicate that CEE effectively inhibits the phosphorylation of ERK, JNK, and p65, subsequently transmitting signals to activate regulatory molecules like c-Fos and NFATc1. NFATc1 has been established as a crucial regulator in osteoclast formation, characterized by its high expression level sustained through self-amplification[41], NFATc1 stimulates osteoclasts to express proteins involved in bone resorption, such as CTSK, MMP9, and TRAP [42]. Our data suggest that CEE treatment decreases the transcriptional activity of NFATc1 and downregulates the expression of its related genes, including *c-Fos*, *Mmp-9*, *Ctsk*, and *Trap*.

In vivo studies utilizing OVX mice were conducted to verify the anti-osteoporotic activity of CEE. Treatment with CEE in these mice led to notable improvements in bone microstructure and a reduction in bone loss. Additionally, bone mass, strength, and the thickness and quantity of bone trabeculae were enhanced. Furthermore, CEE treatment resulted in decreased expression of genes and proteins such as TRAP, CTSK, and MMP-9 in OVX mice, affirming its anti-osteoporotic efficacy. Prior research has shown that the interaction between RANKL and its receptor RANK is pivotal in activating osteoclasts. In contrast, OPG, secreted by osteoblasts, impedes this interaction by binding to RANKL, thus preventing osteoclast differentiation and activation [43]. In this study, we observed that CEE upregulated the levels of E_2 and OPG, while concurrently downregulating RANKL in serum. The balance of these elements plays a crucial role in bone remodeling, potentially influencing the ability of osteoblasts to stimulate osteoclast differentiation and activation, and thereby the degree of bone resorption. These findings suggest that CEE may regulate the OPG/RANKL expression, subsequently affecting the lineage of osteoblasts and stromal cells, and thus the activity of osteoclasts in osteoporosis management. Future research should focus on investigating CEE' s role in the coupling dynamics between osteoclasts and osteoblasts.

In conclusion, our study demonstrates that CEE effectively inhibits the differentiation and activity of osteoclasts induced by RANKL. This effect on RANKL-mediated pathways, such as ERK, JNK, NF-κB, and other downstream factors in osteoclasts, particularly its inhibitory impact on TRAF6, highlights its therapeutic potential. However, this research is not without limitations, and further studies are

needed to explore the detailed mechanisms of interaction between CEE's effects on osteoblasts and osteoclasts. Additionally, our *in vitro* findings indicate that CEE may serve as a potential therapeutic option for osteoporosis and other osteolytic diseases (Fig. S2).

Conclusions

CEE significantly inhibits osteoporosis induced by

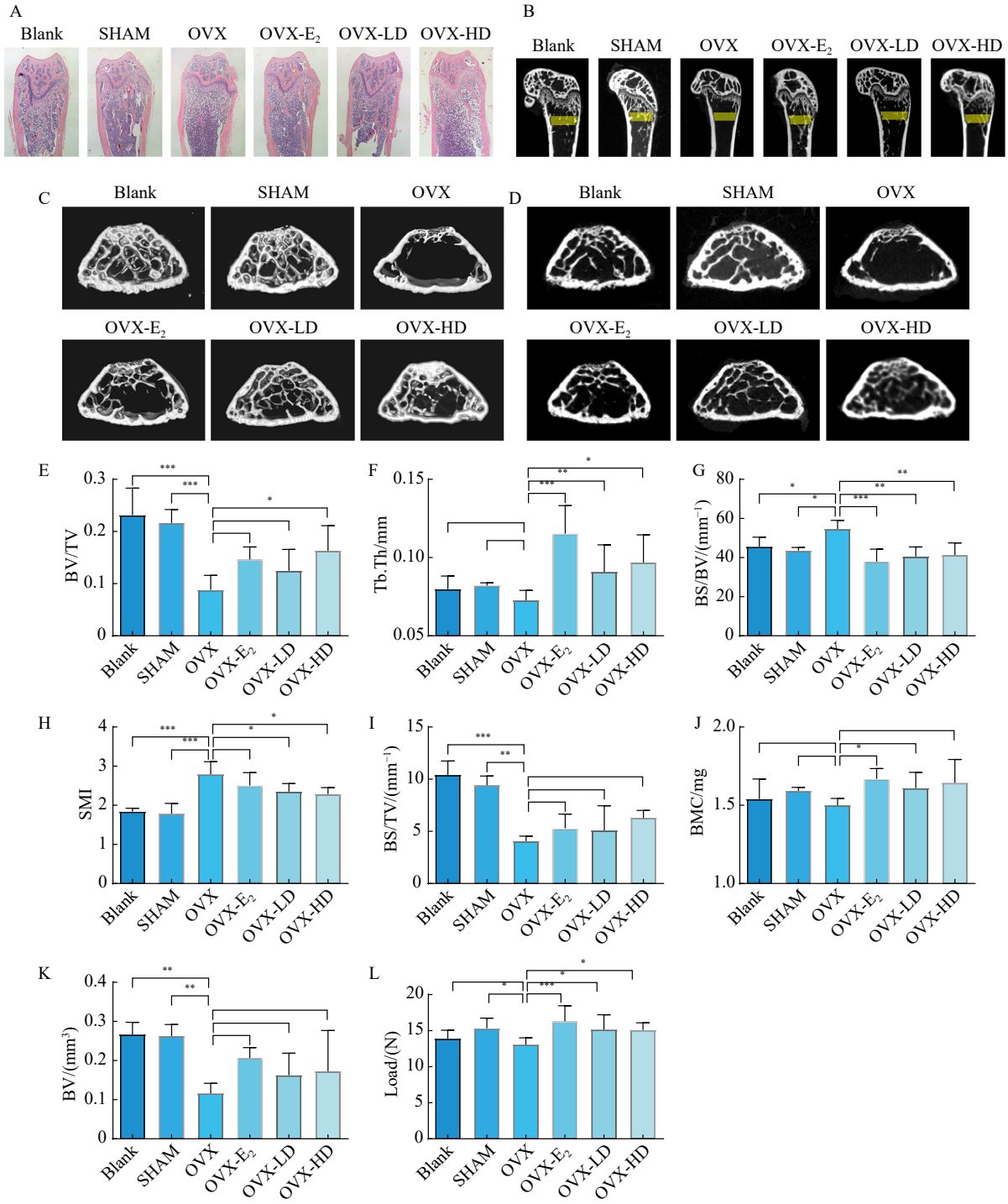

Fig. 5 Stereological parameter of trabecular bone in the mouse femur after CEE treatment analyzed by micro-CT and histological analysis. (A) Histological analysis of tibias with H&E staining. (B) Region of interest (ROI) and longitudinal section. (C) 3D reconstruction pictures of ROI. (D) The intersecting surface of ROI. (E) Bone volume/total volume (BV/TV). (F) Trabecular thickness (Tb.Th). (G) Bone surface/bone volume (BS/BV). (H) Structure model index (SMI). (I) Bone surface/total volume (BS/TV). (J) Bone mineral content (BMC). (K) Bone volume (BV). (L) The maximum load-bearing capacity of each group. Data are expressed as the mean ± SD (n = 6), $^{*}P < 0.05$, $^{**}P < 0.01$, $^{***}P < 0.001$ *vs* OVX group.

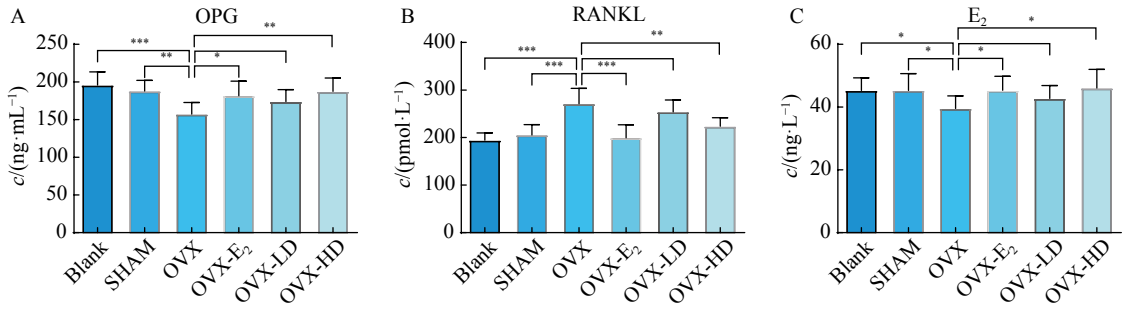

Fig. 6 The effect of CEE on tibia mechanical properties and levels of osteoporosis-related factors in the serum of mice. (A) The level of OPG in serum. (B) The level of RANKL in serum. (C) The level of E_2 in serum. Each sample was repeatedly tested at least three times, $n = 6$. $^{*}P < 0.05$, $^{**}P < 0.01$, $^{***}P < 0.001$ *vs* OVX group.

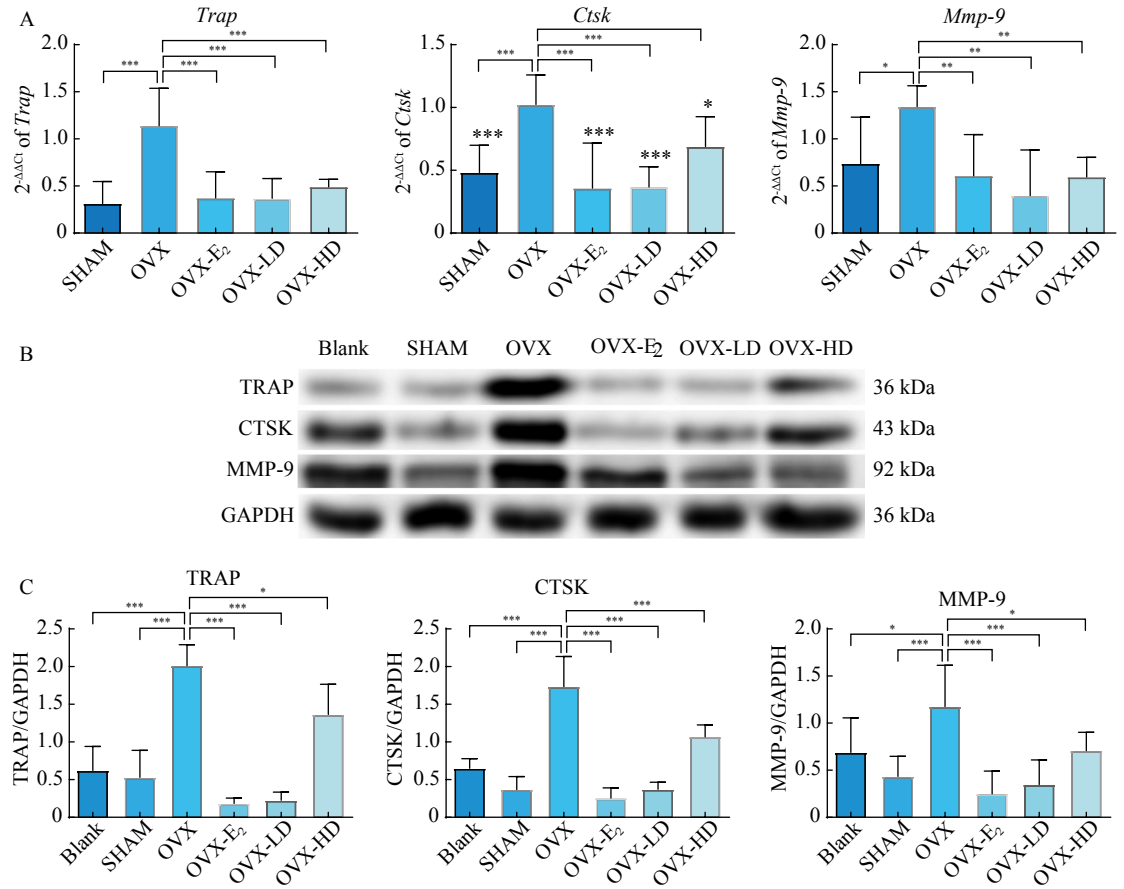

Fig. 7 CEE suppressed the MMP-9, CTSK, and TRAP expressions in the femora of OVX mice. (A) Gene expressions of *Trap*, *Ctsk*, and *Mmp*-9 in femora. (B) WB bands of TRAP, CTSK, MMP-9, and GAPDH. (C) Protein expressions of TRAP, CTSK, and MMP-9 in femora. Each sample was repeatedly tested at least three times, $n = 6$. $^{*}P < 0.05$, $^{**}P < 0.01$, $^{***}P < 0.001$ *vs* OVX group.

ovariectomy in mice, as well as RANKL-induced osteoclast differentiation and bone resorption function. Through its action on the ER/RANK/NFATc1 signaling pathway, CEE suppresses the expression of key proteins including RANK, TRAF6, c-Fos, and NFATc1. It also effectively inhibits the phosphorylation of ERK and JNK within the MAPK pathway, along with the phosphorylation of p65 in the NF-*κ*B pathway. These combined actions contribute to the reduction of osteoclast differentiation and bone resorption activity.

Supplementary Information

Supplementary data to this article can be obtained by sending E-mail to the corresponding authors.

References

[1] Zhi X, Chen X, Su J. Advances in research on the mechanism of postmenopausal osteoporosis [J]. *Chin J Osteoporos*, 2018, **24**(11): 1510-1513, 1534.

[2] Chinese Society of Bone and Mineral Research. Guidelines for the diagnosis and management of primary osteoporosis

(2017) [J]. *Chin J Osteoporos Bone Miner Res*, 2017, **10**(5): 413-443.
[3] Boyce BF, Xing L. Functions of RANKL/RANK/OPG in bone modeling and remodeling [J]. *Arch Biochem Biophys*, 2008, **473**(2): 139-146.
[4] De Vries TJ, Schoenmaker T, Aerts D, *et al*. M-CSF priming of osteoclast precursors can cause osteoclastogenesis-insensitivity, which can be prevented and overcome on bone [J]. *J Cell Physiol*, 2015, **230**(1): 210-225.
[5] Bourette RP, Rohrschneider LR. Early events in M-CSF receptor signaling [J]. *Growth Factors*, 2000, **17**(3): 155-166.
[6] Kim HJ, Kang WY, Seong SJ, *et al*. Follistatin-like 1 promotes osteoclast formation *via* RANKL-mediated NF-Kappa B activation and M-CSF-induced precursor proliferation [J]. *Cell Signal*, 2016, **28**(9): 1137-1144.
[7] Boyce BF. Advances in the regulation of osteoclasts and osteoclast functions [J]. *J Dent Res*, 2013, **92**(10): 860-867.
[8] Poblenz AT, Jacoby JJ, Singh S, *et al*. Inhibition of RANKL-mediated osteoclast differentiation by selective TRAF6 decoy peptides [J]. *Biochem Biophys Res Commun*, 2007, **359**(3): 510-515.
[9] Abdelmagid SM, Sondag GR, Moussa FM, *et al*. Mutation in osteoactivin promotes receptor activator of NF Kappa B ligand (RANKL)-mediated osteoclast differentiation and survival but inhibits osteoclast function [J]. *J Biol Chem*, 2015, **290**(33): 20128-20146.
[10] Basak S, Behar M, Hoffmann A. Lessons from mathematically modeling the NF-Kappa B pathway [J]. *Immunol Rev*, 2012, **246**(1): 221-238.
[11] Ihn HJ, Lee D, Lee T, *et al*. The 1, 2, 3-triazole derivative KP-A021 suppresses osteoclast differentiation and function by inhibiting RANKL-mediated MEK-ERK signaling pathway [J]. *Exp Biol Med*, 2015, **240**(12): 1690-1697.
[12] Amano S, Chang YT, Fukui Y. ERK5 activation is essential for osteoclast differentiation [J]. *PLoS One*, 2015, **10**(4): e0125054.
[13] Lee K, Chung YH, Ahn H, *et al*. Selective regulation of MAPK signaling mediates RANKL-dependent osteoclast differentiation [J]. *Int J Biol Sci*, 2016, **12**(2): 235-245.
[14] Siddiqi MH, Siddiqi MZ, Kang S, *et al*. Inhibition of osteoclast differentiation by ginsenoside Rg3 in RAW264.7 cells *via* RANKL, JNK and P38 MAPK pathways through a modulation of cathepsin K: an *in silico* and *in vitro* study [J]. *Phytother Res*, 2015, **29**(9): 1286-1294.
[15] Choi SW, Park KI, Yeon JT, *et al*. Anti-osteoclastogenic activity of matairesinol *via* suppression of P38/ERK-NFATc1 signaling axis [J]. *BMC Complem Altern M*, 2014, **14**: 35.
[16] Sen B, Styner M, Xie Z, *et al*. Mechanical loading regulates NFATc1 and *β*-catenin signaling through a GSK3β control node [J]. *J Biol Chem*, 2009, **284**(50): 34607-34617.
[17] Shi XD, Miller JS, Harper LJ, *et al*. Reactivation of cocaine reward memory engages the Akt/GSK3/MTOR signaling pathway and can be disrupted by GSK3 inhibition [J]. *Psychopharmacology*, 2014, **231**(16): 3109-3118.
[18] Nagy V, Penninger JM. The RANKL-RANK story [J]. *Gerontology*, 2015, **61**(5): 534-542.
[19] Liu W, Zhang XL. Receptor activator of nuclear factor-Kappa B ligand (RANKL)/RANK/osteoprotegerin system in bone and other tissues [J]. *Mol Med Rep*, 2015, **11**(5): 3212-3218.
[20] An J, Hao D, Zhang Q, *et al*. Natural products for treatment of bone erosive diseases: the effects and mechanisms on inhibiting osteoclastogenesis and bone resorption [J]. *Int Immunopharmacol*, 2016, **36**: 118-131.
[21] Xie BP, Shi LY, Li JP, *et al*. Oleanolic acid inhibits RANKL-induced osteoclastogenesis *via* ER Alpha/MiR-503/RANK signaling pathway in RAW264.7 cells [J]. *Biomed Pharmacother*, 2019, **117**: 109045.
[22] Chinese Pharmacopoeia Commission. *Pharmacopoeia of the People's Republic of China* [S]. Science and Technology Press of Shanghai, 2020: 39.
[23] Huang YL, Wang SS, Liu L, *et al*. Review of traditional uses, botany, chemistry, pharmacology, pharmacokinetics, and toxicology of Radix Cyathulae [J]. *Chin Med*, 2019, **14**(1): 17.
[24] Wang Y, Zhou GJ, Yan ZX, *et al*. Estrogen effect of *Cyathnla capitata* Moq. in ovariectomized rats *in vivo* and its impact on lipid metabolism [J]. *Mat Child Health Care China*, 2015, **30**(29): 5063-6.
[25] Wang Y, Zhou GJ, Yan ZX, *et al*. The protective effect of *Cyathula officinalis* Kuan on bone in ovariectomized rats [J]. *Chin J Osteoporos*, 2015, **21**(8): 918-921.
[26] Wang YY, Zhang XQ, Yuan FF, *et al*. Research on the anti-inflammatory and immunodulatory activity of Cyathulae Radix and Achyranthis Bidentatae Radix polysaccharides [J]. *J Jining Med Univ*, 2018, **41**(2): 132-134.
[27] Ji QL, Kong XD, Qi SH, *et al*. The experimental study of cyasterone on the treatment of osteoporosis through the bidirectional effect of inhibiting osteoclast differetiation and promoting osteoblast differentiation [J]. *J Kunming Med Univ*, 2018, **39**(5): 21-28.
[28] Xie JC, Zhao Y, Huang LH, *et al*. Cupatosterone inhibits osteoclastic differentiation through estrogen-like effects [J]. *Central South Pharm*, 2022, **20**(9): 2046-2051.
[29] Yan WJ, Zhong YY, Wang H, *et al*. Quantitative analysis of triterpenoid saponins in *Cyathula officinalis* by HPLC-ELSD [J]. *Pharm Clin Res*, 2014, **22**(4): 336-338.
[30] Feng HB, Du XG, Liu J, *et al*. Novel polysaccharide from Radix *Cyathulae officinalis* Kuan can improve immune response to ovalbumin in mice [J]. *Int J Biol Macromol*, 2014, **65**: 121-128.
[31] Li M, Hao L, Li L, *et al*. Cinnamtannin B-1 prevents ovariectomy-induced osteoporosis *via* attenuating osteoclastogenesis and ROS generation [J]. *Front Pharmacol*, 2020, **11**: 1023-1036.
[32] Li J, Liang J, Wu L, *et al*. CYT387, a JAK-specific inhibitor impedes osteoclast activity and oophorectomy-induced osteoporosis [J]. *Front pharmacol*, 2022, **13**: 829862-8299880.
[33] Liu S, Zhou H, Liu H, *et al*. Fluorine-contained hydroxyapatite suppresses bone resorption through inhibiting osteoclasts differentiation and function *in vitro* and *in vivo* [J]. *Cell Proliferat*, 2019, **52**(3): e12613-12624.
[34] Tzeng HE, Huang PH, Tsai CH, *et al*. Isosteviol derivative inhibits osteoclast differentiation and ameliorates ovariectomy-induced osteoporosis [J]. *Sci Rep*, 2018, **8**(1): 11190-11212.
[35] He JB, Chen MH, Lin DK. New insights into the tonifying kidney-yin herbs and formulas for the treatment of osteoporosis [J]. *Arch Osteoporos*, 2017, **12**(1): 1-14.
[36] He J, Li X, Wang Z, *et al*. Therapeutic anabolic and anticatabolic benefits of natural Chinese medicines for the treatment of osteoporosis [J]. *Front Pharmacol*, 2019, **10**: 1344.
[37] Wang T, Liu Q, Tjhioe W, *et al*. Therapeutic potential and outlook of alternative medicine for osteoporosis [J]. *Curr Drug Targets*, 2017, **18**(9): 1051-1068.
[38] Suvarna V, Sarkar M, Chaubey P, *et al*. Bone health and natural products−an insight [J]. *Front Pharmacol*, 2018, **9**: 981.
[39] Meng JH, Zhang WK, Wang C, *et al*. Catalpol suppresses osteoclastogenesis and attenuates osteoclast-derived bone resorption by modulating PTEN activity [J]. *Biochem Pharmacol*, 2020, **171**: 113715.
[40] Stemig M, Astelford K, Emery A, *et al*. Deletion of histone deacetylase 7 in osteoclasts decreases bone mass in mice by interactions with MITF [J]. *PLoS One*, 2015, **10**(4): e0123843.
[41] Swarnkar G, Chen TH, Arra M, *et al*. NUMBL interacts with TAK1, TRAF6 and NEMO to negatively regulate NF-*κ*B signaling during osteoclastogenesis [J]. *Sci Rep*, 2017, **7**(1): 12600-12610.
[42] Hamid A, Song J, Thakur N, *et al*. TGF-β promotes PI3K-AKT signaling and prostate cancer cell migration through the TRAF6-mediated ubiquitylation of p85α [J]. *Sci Signal*, 2017, **10**(486): 1-15.
[43] Abdallah BM, Stilgren LS, Nissen N, *et al*. Increased RANKL/OPG MRNA ratio in iliac bone biopsies from women with hip fractures [J]. *Calcif Tissue Int*, 2005, **76**: 90-97.

Cite this article as: SHI Liying, REN Liuyi, LI Jinping, LIU Xin, LU Jingjing, JIA Lujuan, XIE Baoping, TANG Siyuan, LIU Wei, ZHANG Jie. Ethanol extract of Cyathulae Radix inhibits osteoclast differentiation and bone loss [J]. *Chin J Nat Med*, 2024, **22**(3): 212-223.